

Magnetic Lineations in the Ancient Crust of Mars

J. E. P. Connerney,^{1*} M. H. Acuña,¹ P. J. Wasilewski,¹ N. F. Ness,²
H. Rème,³ C. Mazelle,³ D. Vignes,³ R. P. Lin,⁴ D. L. Mitchell,⁴
P. A. Cloutier⁵

The Mars Global Surveyor spacecraft, in a highly elliptical polar orbit, obtained vector magnetic field measurements above the surface of Mars (altitudes >100 kilometers). Crustal magnetization, mainly confined to the most ancient, heavily cratered martian highlands, is frequently organized in east-west-trending linear features, the longest extending over 2000 kilometers. Crustal remanent magnetization exceeds that of terrestrial crust by more than an order of magnitude. Groups of quasi-parallel linear features of alternating magnetic polarity were found. They are reminiscent of similar magnetic features associated with sea floor spreading and crustal genesis on Earth but with a much larger spatial scale. They may be a relic of an era of plate tectonics on Mars.

The Mars Global Surveyor (MGS) magnetometer experiment (1) acquires continuous vector magnetic field measurements at a rate of up to 32 samples per second throughout much of the MGS mission, including during repeated low-altitude passes through the atmosphere ("aerobraking") designed to circularize the spacecraft orbit by atmospheric drag (2). The spacecraft has been in a nearly polar, high inclination orbit since September 1997. The observations most useful for the study of magnetic sources in the crust of Mars were acquired within about 10 min of periapsis, during which time the spacecraft altitude dropped below 200 km to as low as 101 km. Each pass provides useful data over a range of about $\pm 25^\circ$ latitude and a narrow range of longitudes centered on the latitude and longitude of periapsis. During the nearly 18 months of aerobraking operations, the latitude of periapsis has evolved essentially from pole to pole, providing globally distributed but sparse coverage of the planet (3).

Acuña *et al.* (4), working with northern midlatitude data available early in the mission, reported the discovery of multiple magnetic sources in the crust of Mars, the largest of which had an estimated magnetic moment of $\sim 1.6 \times 10^{16}$ A-m². They also reported that at least one source, near 32.8°N and 23.6°W, appeared to be part of an extended linear feature striking approximately east-west. More recent observations, which covered the southern hemisphere (3), showed that the most intense magnetic sources lie in

the Terra Cimmeria and Terra Sirenum, straddling 180°W at mid to high southern latitudes. Many of these features also appear linearly extended in the east-west direction, nearly perpendicular to the MGS orbital plane. We concentrate our analysis on a subset of the MGS observations acquired over the southern hemisphere and within $\pm 60^\circ$ longitude of the 180°W longitude meridian.

Unlike terrestrial aeromagnetic surveys, conducted at constant altitude, our survey is a compilation of orbit segments dipping below the ionosphere (Fig. 1). Survey tracks begin and end with the spacecraft at an altitude of 200 km, and the minimum altitude is achieved midtrack, usually in the range of 103 to 110 km. The maximum spatial resolution of the measurements is achieved at lowest altitude. Adjacent tracks may appear dissimilar, even crossing the same structure, if the altitude difference is appreciable. The measured field at higher altitudes will be relatively weaker and may appear as a smoothed and attenuated copy of the adjacent track. Some of the track-to-track differences can be reconciled by taking note of where each track begins and ends, as an indication of altitude.

The most important sources of crustal magnetization in the survey region are organized in extensive, east-west-trending linear features. The prominent positive radial magnetic feature near 53°S and centered on the 180° meridian can be followed over 2000 km; quasi-parallel features nearby can be traced for 1000 km. It also appears that intense positive radial linear features are separated by equally intense negative radial linear features, suggesting bands of crustal remanent magnetization of alternating sign. We model a representative set of individual survey tracks to explore models of crustal magnetization that are consistent with the observations.

Our measurements of the vector magnetic

field of the martian crust (Fig. 2) are unlike those available on Earth. Earth's large global magnetic field (30,000 to 60,000 nT), generated by dynamo action in the fluid outer core, makes it difficult to measure the relatively small signal due to crustal sources. In common practice, only that component of the crustal field parallel to the global field can be accurately measured. The polarity of the field attributed to crustal sources is difficult to establish because one must first remove the global field and what remains depends on how much global field is removed. In contrast, at Mars, there (presently) is no global field, and the vector magnetic field of crustal sources can be measured directly. Terrestrial anomalies may be attributed to induced or remanent magnetism or some combination of both. Historically, terrestrial anomalies have most often been attributed to induced magnetization, which persists only in the presence of the inducing field. It is difficult to distinguish between induced or remanent crustal magnetization in Earth's crust without sampling the rocks or removing the inducing field. In contrast, the martian crustal field may be unambiguously attributed to remanent magnetism because there is no inducing field. A terrestrial aeromagnetic or marine survey at low altitude might find perturbations in the ambient field as large as ~ 1000 nT over distances of a few to tens of kilometers. The largest magnetic anomalies on Earth produce a variation of ± 10 nT at satellite altitude of about 400 km (5). In contrast, the magnetometer on MGS measured ± 1500 nT at >100-km altitude, with a spatial scale of ~ 200 km, all of it due to crustal remanent magnetism. At 400-km altitude, these martian crustal sources produce fields of about ± 200 nT; they dwarf their terrestrial counterparts.

It is not possible to uniquely determine crustal magnetization with even the highest quality vector observations distributed about the source. One can, however, make reasonable assumptions about the sources and find solutions consistent with the observations and assumptions. We assumed that the sources of magnetization can be represented by a group of 20 uniformly magnetized strips of 200 km in width and 30 km in depth, infinitely extended along \hat{y} (east-west). The width chosen is consistent with the maximum spatial resolution expected based on the satellite altitude. The magnetic field of each uniformly magnetized strip was computed with Talwani's thin sheet approximation (6), which is valid as long as the plate thickness is small compared with the distance to the observer. We constrain the product of the plate thickness and the volume magnetization, so, for example, a 10-km-thick plate would require three times the volume magnetization of a 30-km-thick plate. The x and z components of the observed magnetic field are fit to one crustal

¹NASA Goddard Space Flight Center, Greenbelt, MD 20771, USA. ²Bartol Research Institute, University of Delaware, Newark, DE 19716, USA. ³Centre d'Etude Spatiale des Rayonnements, 31028 Toulouse Cedex 4, France. ⁴Space Sciences Laboratory, University of California, Berkeley, CA 94720, USA. ⁵Department of Space Physics and Astronomy, Rice University, Houston, TX 77005, USA.

*To whom correspondence should be addressed.

REPORTS

magnetization model, parameterized by the volume magnetization (J_x and J_z) of each of the 20 thin plates. The magnetic field associated with the y component of a uniformly magnetized source of infinite extent in y is zero, so J_y cannot be constrained by measurements of the field exterior to such a source.

A generalized inverse methodology (7) is used to find solutions that fit the observations by minimizing the root mean squared (RMS) residual between model and observations. We formed an N observations by M parameters matrix of partial derivatives relating each observation to the model parameters, performed a singular value decomposition of that matrix, and constructed solutions by the summation of eigenvectors (linear combinations of the original parameters). These solutions are well determined in a mathematical sense, under our assumptions, with matrices characterized by modest ratios of maximum and minimum eigenvalues (30 to 100). However, adoption of different assumptions, say, the number, width, or absolute positions of the uniformly magnetized plates, can result in different magnetizations; our solutions are representative and by no means unique. Furthermore, it is expected that the physical dimensions of the sources are considerably

more complex than assumed here and that the volume magnetizations are nonuniform, reflecting spatial differences in mineralogy, magnetic microstructure, and history.

The best fitting model (Fig. 2) fits the observations in \hat{x} and \hat{z} components with an RMS residual of 45 nT. The corresponding crustal magnetization shows variation on a scale of a few hundred kilometers, with magnetization per unit volume approaching about ± 20 A/m in J_x and J_z . Several reversals in the direction of magnetization are inferred for both components of the magnetization (8). Observations acquired on an earlier pass, P5, DOY 13, 1999 (Fig. 3), just 2° eastward (72 km) of those acquired on DOY 15 (Fig. 2), fit our model with an RMS residual of 28 nT. The attenuation of features from the pass on DOY 13 toward large negative \hat{x} and the increased structure observed toward large positive \hat{x} are consistent with the more northerly location of periapsis for this orbit compared with DOY 15. Despite the differences, the crustal magnetization inferred from these two passes is similar in magnitude and sign.

Another pair of periapsis passes over the same structure on DOY 20 (Fig. 4) and DOY 6 (Fig. 5) of 1999, separated by about 3° longitude (108 km), fit our model with RMS

residuals of 49 and 41 nT, respectively. The difference in latitude of periapsis (68.0°S for DOY 20 and 34.6°S for DOY 6) and therefore altitude leads to differences in the measured magnetic field. DOY 20 observations showed high-amplitude, high-spatial resolution features toward $-\hat{x}$, where the lowest altitudes were obtained; the DOY 6 observations show high-amplitude, high-spatial resolution features toward $+\hat{x}$, where the lowest altitudes were obtained on this pass. Reversals in the direction of magnetization are common to both models, particularly in \hat{z} , where reversals are found with a scale length of 200 km along \hat{x} (limiting spatial resolu-

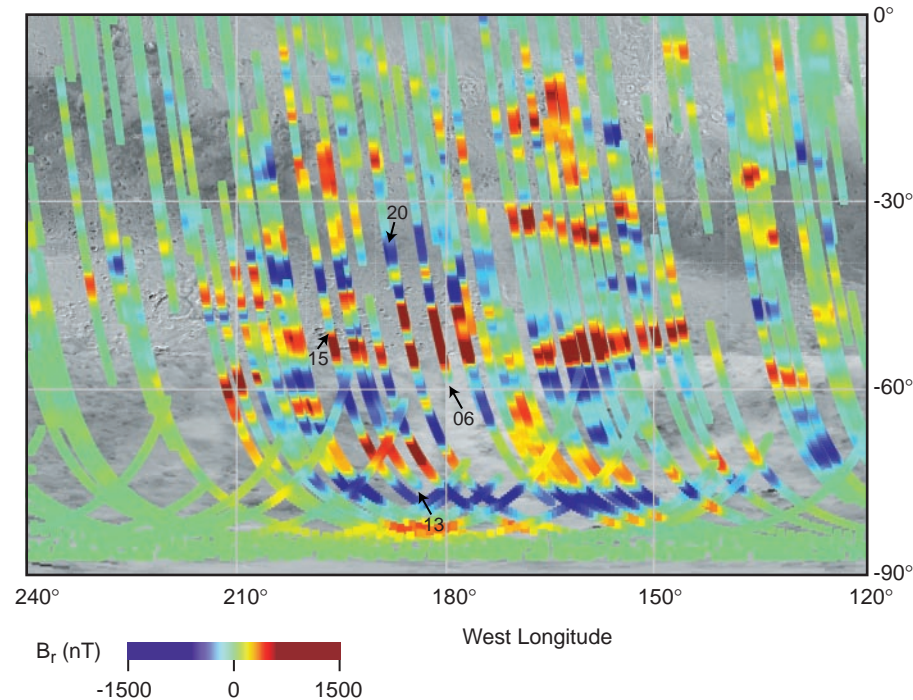


Fig. 1. Latitude-longitude map of one-third of the southern hemisphere of Mars. Subsatellite latitude and longitude for each periapsis are indicated by a largely north-south line segment representing that part of the orbit below 200-km altitude. The color of each segment represents the radial component of the magnetic field (B_r) measured by MGS at that location without correction for the variation of satellite altitude (200 km $< r <$ 103 km). The radial field component within the survey area ranged from -1389 nT (blue) to 1476 nT (red). A stretched color bar is used to partially compensate for altitude variation; this method of display emphasizes the sign of B_r rather than the magnitude, which is strongly dependent on distance from the source (26). Where two tracks overlap, the latest track, with a more southerly latitude of periapsis, appears overprinted on the earlier track.

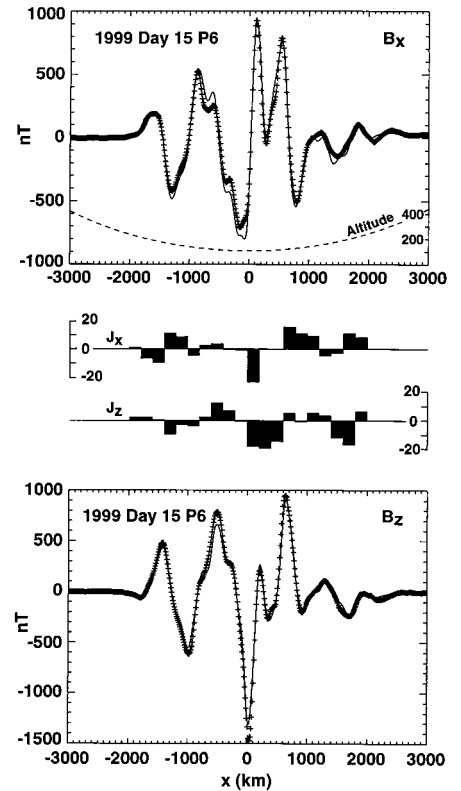


Fig. 2. Plot of the vector magnetic field measured during aerobraking, or periapsis pass (P) 6, on calendar day of year (DOY) 15, 1999. Periapsis occurred at 54.5°S , 196.1°W and 107-km altitude. The x (positive north) and z (positive down) components of the vector field [B_x (top) and B_z (bottom)], resampled at 3-s intervals, are plotted as symbols (crosses). The solid line is a model fit to the observations. The y component of the field (not shown) is less than the x and z components, consistent with a source greatly extended in the y direction (east-west). The observations are plotted as a function of distance (x) north and south of the origin, in each case located on the surface at 53°S and at the longitude of periapsis. Altitude variation in kilometers is indicated by the dashed line. The x and z components of the model crustal magnetization per unit volume (J_x and J_z , in units of amperes per meter) are indicated in the bar graph between the two panels.

REPORTS

tion). An attempt to increase the spatial resolution of the model to 100 km along x resulted in excessive covariability of model parameters (magnetization per unit volume) between adjacent bands, that is, limited improvement in spatial resolution. A model fit to the combined data set (Fig. 6) fits DOY 20 and DOY 6 observations nearly as well (RMS residual = 69 nT) as the individual data sets and is similar to that shown in Fig. 4.

These observations are consistent with a crustal magnetization model made up of multiple quasi-parallel linear features with dimensions of ≥ 200 km in width, extending as far as 2000 km in length and with volume magnetization (assuming a 30-km-thick source) of ± 20 A/m. Reversals in the direction of magnetization of adjacent bands are common if not the rule. It is also possible that in assuming 200-km-wide bands, we have averaged over narrower bands ($\ll 200$ km) of alternating magnetization that we do not have sufficient resolution to detect. If so, the magnetization per unit volume would have to be much greater than that averaged over 200 km, which is already very large. Assuming a 2000-km length, the total magnetic moment of just one 200-km-wide band with magnetization of 20 A/m is 2.4×10^{17} A-m². This is an order of magnitude greater moment than that associated with one of the largest mag-

netic anomalies on Earth, the Kursk anomaly in Russia (9).

The Mars highlands crust is on average an order of magnitude more intensely magnetized than terrestrial continental crust (10). The martian crust may have been magnetized by thermoremanent magnetization (TRM), acquired when a rock cools below a critical temperature (Curie temperature) in the presence of a magnetizing field. TRM is an efficient mechanism for producing intense remanence in a relatively weak inducing field such as that expected on the surface of a planet with an active dynamo in its deep interior (early Mars or present-day Earth). The magnitude of magnetization acquired by the rock depends critically on the mineralogy, magnetic microstructure, and magnetizing field intensity. Subsequent chemical, thermal, and mechanical processes can alter rock magnetization, so the magnetic properties of the rock depend critically on its history after initial magnetization. The intense magnetization of the martian crust favors mineralogies and microstructures with high TRM, such as multidomain hematite or pyrrhotite, over multidomain magnetite (11). Hematite has been identified on the martian surface by the thermal emission spectrometer on MGS (12). It also implies a relatively intense inducing field, comparable to or greater than that of Earth. The intense magnetization of the mar-

tian crust is consistent with the high iron content (17% by weight Fe) found in soils at the Pathfinder landing site (13) and in the martian meteorites (15 to 30%) (14) relative to terrestrial continental crust (a few percent). This is consistent with less differentiation of the Mars highlands crust and presumably mantle relative to Earth.

Not all of the magnetization in the martian crust that has survived to the present day is organized into linear features (3). Similar bands of alternating magnetization are also found in the northern hemisphere, within and south of Acidalia Planitia. On Earth, magnetic lineations of alternating polarity are found in oceanic crust and are associated with sea floor spreading and repeated reversals of the dipole field (15, 16). The discovery of such features on Earth led to the widespread acceptance of the unifying theory of plate tectonics, the movement of large, thin, rigid plates about the surface of Earth in response to mantle convection. Mid-ocean ridge spreading centers occur between two plates that are being pulled apart. Molten material from below fills the void, cools below its Curie temperature, and acquires a permanent remanent magnetic moment aligned with the terrestrial dipole field. New crustal material is continuously generated in this process, which, combined with the periodic reversal of Earth's dipole magnetic field, leads to a series of linear features of alternating magnetic polarity aligned

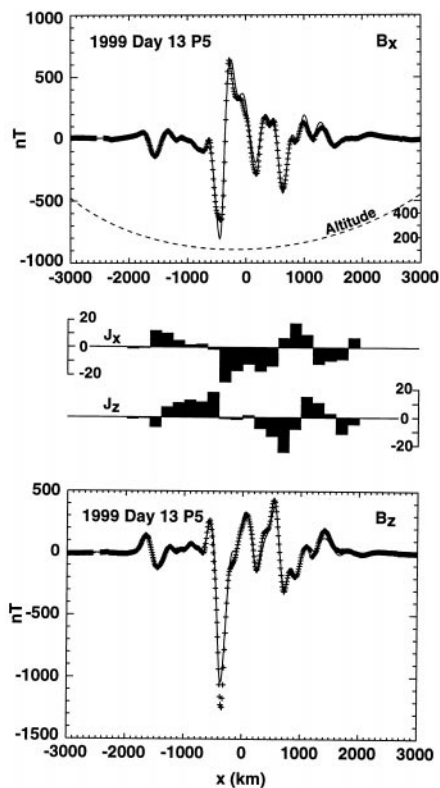


Fig. 3. As in Fig. 2, but for 1999 DOY 13 P5 with periapsis at 49.6°S, 194.2°W and 107-km altitude.

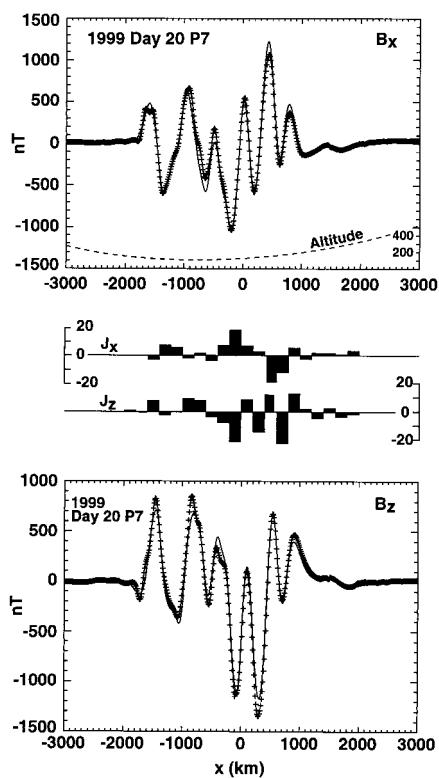


Fig. 4. As in Fig. 2, but for 1999 DOY 20 P7 with periapsis at 68.0°S, 181.2°W and 106-km altitude.

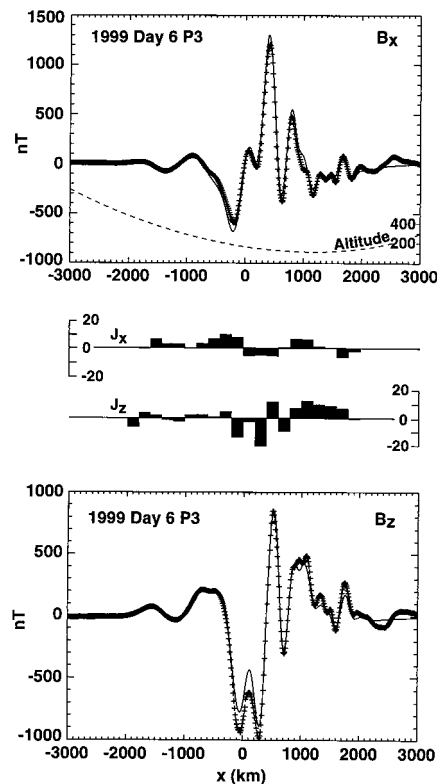


Fig. 5. As in Fig. 2, but for 1999 DOY 6 P3 with periapsis at 34.6°S, 184.3°W and 110.5-km altitude.

with the ridge axis. On Earth, plates spread at a rate of a few centimeters per year, and the dipole reverses at a rate of a few reversals per million years (17), leading to a characteristic horizontal scale length of order 10 km for the width of features magnetized in normal, or reversed, polarity. It is generally believed that although mantle convection occurs in all large bodies, plate tectonics is unique to Earth (18).

By analogy with Earth, sea floor spreading (19) on Mars could have produced magnetic lineations of alternating polarity with a characteristic horizontal scale length of order 100 km if the spreading rate exceeded the contemporary terrestrial rate or if the rate of dipole reversals on Mars was much less than that at Earth. Sleep (20) proposed that the relatively young, northern martian lowlands were produced by sea floor spreading and constructed a plate tectonic model to account for the crustal dichotomy. He estimates that sea floor spreading on Mars occurred at a higher rate than that on Earth, because, in part, of lower gravity (0.38 that of Earth) and slightly greater density of the mantle. Sleep's estimate of rapid sea floor spreading on Mars (about 8 cm/year) is generally consistent with the relatively large scale length of magnetization reversals found in the highlands crust, assuming that the rate of field reversals for Mars and Earth is comparable. However, we note that there is considerable variability in spreading rates on Earth and even more variability in the magnetic field reversal rate throughout history (17).

The most straightforward interpretation of the magnetic lineations in the Mars highland crust is that they formed early in the planet's evolutionary history (early to mid Noachian) by plate tectonics and sea floor spreading, analogous to terrestrial oceanic crust. The Mars highlands would then be viewed as one or more remnants of early "oceanic" crust, reworked in places by subsequent major impacts and thermal events, but preserving, elsewhere, the magnetic imprint acquired when it formed by sea floor spreading. As such, the magnetic record surviving in the highlands crust is a record of the early Mars dynamo, now extinct, and a record of the early thermal evolution of the planet. Plausible alternatives to this interpretation are few. It is possible for a series of vol-

canic or intrusive events to assume the appropriate geometry, that of multiple quasi-parallel linear features, but it is unlikely that they could form with the volume of material necessary, nor is it likely they would acquire alternating magnetization. The latter imposes a requirement for synchronicity with the reversals of the magnetic field. Alternatively, one might suppose that the crust was magnetized uniformly and acquired apparent magnetization reversals by periodic folding, deemed unlikely because of the regularity and scale length required. Finally, it is also possible that the martian crust was magnetized by chemical remanent magnetization (CRM) instead of TRM. Acquisition of CRM occurs at low temperatures as superparamagnetic mineral grains grow to a critical size and, like TRM, can result in intense magnetization, particularly for multidomain hematite or pyrrhotite (11). Banded magnetic formations might be attributed to banded zones of hydrochemical alteration in the martian crust, but it remains difficult to explain bands of alternating magnetization.

The evidence for sea floor spreading on Earth (15) grew ever stronger when the symmetry of the magnetic lineations about the ridge axis was firmly established (16) and when the pattern of normal and reverse magnetization could be compared with a magnetic reversal history compiled independently (21). If we interpret the observations reported here within the context of sea floor spreading, we require at a minimum a ridge axis and plate motion away from that axis in the presence of a reversing magnetic field. Very complicated patterns of magnetic lineations arise on Earth because of transform faulting (22), the presence of multiple ridges, and variable spreading rates (16). Observation of symmetry about an axis would strengthen the argument considerably. However, portions of the Mars highlands crust have undergone substantial reworking (impact and thermal events and fragmentation) subsequent to the acquisition of a magnetic imprint, so the magnetic record on Mars may be less well preserved than the terrestrial example. If these magnetic lineations in the Mars highland crust are a relic of plate tectonics, then a new and familiar paradigm—plate tectonics—must be substituted for the "single plate" paradigm now favored for the planet Mars (23–25).

There is no evidence, at present, of large-scale extensional or compressive tectonics in this region (23) and, in particular, no evidence of transform faulting usually associated with sea floor spreading on Earth. However, this is not surprising, as the great majority of tectonic features deduced from images are associated with the Tharsis region and the increased crustal load of relatively recent volcanics. Surface features associated with a plate tectonic origin of the magnetic lineations would have been obliterated by

subsequent meteorite bombardment. With few visible clues, identification of multiple plates, transform faulting, and other signatures of plate tectonics on Mars may require exploration methods capable of peering deep into the crust, such as magnetic and gravity surveys, electromagnetic remote sensing, and seismic surveys.

References and Notes

1. M. H. Acuña *et al.*, *J. Geophys. Res.* **97**, 7799 (1992).
2. A. L. Albee, F. D. Palluconi, R. E. Arvidson, *Science* **279**, 1671 (1998).
3. M. H. Acuña *et al.*, *ibid.* **284**, 790 (1999).
4. M. H. Acuña *et al.*, *ibid.* **279**, 1676 (1998).
5. R. A. Langel, J. D. Phillips, R. J. Horner, *Geophys. Res. Lett.* **9**, 269 (1982); R. A. Langel, C. C. Schnetzler, J. D. Phillips, R. J. Horner, *ibid.*, p. 273. Note that satellites are placed in circular orbit about Earth at altitudes in excess of about 350 km to prevent rapid orbit decay due to atmospheric drag. Terrestrial magnetic mapping is thus confined to altitudes below about 25 km and above 350 km. A magnetic survey (by balloon) over the Kursk anomaly at 9- and 25-km altitudes measured peak-to-peak amplitudes of 3000 and 1500 nT, respectively. See Y. P. Tsvetkov, N. M. Rotanova, V. N. Oraevsky, S. D. Odintsov, *J. Geomagn. Geoelectr.* **49**, 689 (1997).
6. M. Talwani, *Geophysics* **30**, 797 (1965).
7. J. E. P. Connerney, *J. Geophys. Res.* **86**, 7679 (1981).
8. The magnetic field external to a uniformly magnetized plate of infinite extent is zero, so one may, by superposition of such a plate, construct additional models that fit the observations equally well. For this reason, the direction of magnetization is less well constrained than the change in direction, or magnetization contrast, along \hat{x} .
9. D. N. Ravat, W. J. Hinze, P. T. Taylor, *Tectonophysics* **220**, 157 (1993). Terrestrial anomalies are most often attributed to induced magnetism. Estimates of the moments associated with the largest terrestrial anomalies vary but are about 1 to 2×10^{16} A-m².
10. We compare Mars' crustal magnetization with an equivalent layer magnetization model of terrestrial continental crust derived from satellite observations. See, for example, M. A. Mayhew and S. C. Gallier, *Geophys. Res. Lett.* **9**, 311 (1982).
11. D. A. Clark, *Bull. Aust. Soc. Explor. Geophys.* **14**, 49 (1983). Magnetite has traditionally been the favorite candidate for terrestrial magnetic anomalies, because of its much greater magnetic susceptibility compared with other magnetic minerals. This view reflects the prevailing assumption that induced magnetization dominates remanent magnetization in terrestrial magnetic anomalies. However, if terrestrial crustal magnetism is attributed to remanent magnetism, multidomain hematite or pyrrhotite mineralogies would also be favored over multidomain magnetite, characterized by relatively weak TRM, for Earth's crustal magnetism.
12. M. D. Lane, R. V. Morris, P. R. Christensen, *Lunar Planet. Sci. Conf.* **30** (1999) [CD-Rom].
13. R. Rieder *et al.*, *Science* **278**, 1771 (1997).
14. H. Y. McSween, *Rev. Geophys.* **23**, 391 (1985).
15. F. J. Vine and D. H. Matthews, *Nature* **199**, 4897 (1963).
16. W. C. Pitman III and J. R. Heirtzler, *Science* **154**, 1164 (1966).
17. R. T. Merrill and M. W. McElhinny, *The Earth's Magnetic Field* (Academic Press, London, 1983), p. 140.
18. G. Schubert, *Encyclopedia of Planetary Sciences*, J. H. Shirley and R. W. Fairbridge, Eds. (Chapman & Hall, London, 1997), p. 416.
19. The term "sea floor spreading," as used here, refers to the genesis of new crust at a spreading center, or along a ridge axis, by plate tectonics and is not intended to imply the existence of a sea or ocean on Mars. On Earth, spreading centers are found in oceans, an association that is reflected in the terminology. Water is thought to play a central role in plate tectonics, however, because of its importance in melting, heat transfer, and mechanical properties.

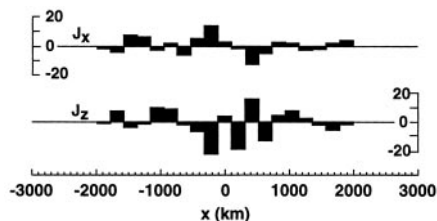


Fig. 6. A bar graph of the model magnetization per unit volume (in amperes per meter) resulting from a fit to the combined data set for DOY 20 P7 and DOY 6 P3.

20. N. H. Sleep, *J. Geophys. Res.* **99**, 5639 (1994).
 21. F. J. Vine and J. T. Wilson, *Science* **150**, 485 (1965).
 22. J. T. Wilson, *Nature* **207**, 343 (1965); *Science* **150**, 482 (1965).
 23. W. B. Banerdt, M. P. Golombek, K. Tanaka, in *Mars*, H. H. Kieffer, B. M. Jakosky, C. W. Snyder, M. S. Matthews, Eds. (Univ. of Arizona Press, Tucson, AZ, 1992), pp. 249–297.
 24. R. O. Pepin and M. H. Carr, in *Mars*, H. H. Kieffer, B. M. Jakosky, C. W. Snyder, M. S. Matthews, Eds. (Univ. of Arizona Press, Tucson, AZ, 1992), pp. 120–143.
 25. G. Schubert, S. C. Solomon, D. L. Turcotte, M. J. Drake, N. H. Sleep, in *ibid.*, pp. 147–183.
 26. The magnetic field of a point source, dipole, or equiv-

alently a uniformly magnetized sphere varies as $1/r^3$, where r is the distance to the source. The field of an infinite line of dipoles, or equivalently a uniformly magnetized infinite cylinder, varies as $1/r^2$, where r is the distance to the source along the line perpendicular to the source joining source and observer. See, for example, R. J. Blakely [*Potential Theory in Gravity and Magnetic Applications* (Cambridge Univ. Press, Cambridge, 1995)].
 27. We thank the many Mars Global Surveyor Project personnel, Goddard Space Flight Center engineering and technical staff, and our colleagues at the University of California at Berkeley and the Centre d'Etude Spatiale des Rayonnements, Toulouse, France, who

have contributed to the success of the Magnetometer and Electron Reflectometer Investigation. We thank M. Kaelberer, D. Brain, F. Perin, and P. Lawton for their participation in data analysis and display and C. Ladd for graphics and presentation support. We also acknowledge helpful reviews and comments by M. Purucker, J. Heirtzler, G. Kletetschka, T. Ravat, and others. G. Kletetschka and M. Purucker are acknowledged for extensive discussions regarding magnetic mineralogy. The research at Berkeley was supported by NASA grant NAG-5-959. N.F.N. acknowledges support in part by NASA grant NAG-5-3538.

15 March 1998; accepted 9 April 1999

Neck Posture and Feeding Habits of Two Jurassic Sauropod Dinosaurs

Kent A. Stevens¹ and J. Michael Parrish²

Articulated digital reconstructions of two diplodocid sauropods revealed cervical poses and feeding envelopes. The necks of *Diplodocus* and *Apatosaurus* were nearly straight but gently declined such that the heads, which were themselves angled downward relative to the neck, were close to ground level in their neutral, undeflected posture. Both necks were less flexible than conventionally depicted, and *Diplodocus* was less capable of lateral and dorsal curvature than *Apatosaurus*. The results suggest that these sauropods were adapted to ground feeding or low browsing, contrary to the view that diplodocid sauropods were high browsers.

The fauna of the Late Jurassic Morrison Formation was dominated by huge, long-necked sauropod dinosaurs. At least six genera occur in the Morrison and five genera occur, apparently sympatrically, in the main quarry at Dinosaur National Monument (1, 2). The abundance, size, and diversity of sauropods suggest that they played a central role in the Morrison and other continental ecosystems of the Jurassic and Cretaceous.

The key to understanding the feeding strategies of sauropods lies in the biomechanics of their elongate necks. When first described (3, 4), *Diplodocus* was depicted with a neck that was nearly horizontal, or sloping down with a gentle dorsal arch (5, 6). Recently, *Diplodocus* and other sauropods have been restored (7–9) with their heads far above ground level, with a sharp, swanlike dorsiflexion in the neck. Additionally, several taxa were depicted in a tripod (hind limbs plus tail) pose (7, 9). These inferences of near-vertical necks in sauropods have sparked a lively debate (10–12) about how the sauropod circulatory system pumped blood to the elevated head; this has yielded such creative suggestions as the presence of multiple hearts in the diplodocid *Barosaurus* (12).

It is difficult to evaluate these alternative

hypotheses by direct manipulation (13) of the original specimens because their fossil remains are too awkward, heavy, and fragile to move in articulation manually. In addition, postdepositional distortion often prevents proper articulation. As an alternative, we chose to manipulate detailed digital models of sauropod skeletons with an interactive graphics software package (14) for constructing and articulating three-dimensional (3D) models of dinosaur skeletons. The entire axial skeleton and the major elements of the appendicular skeleton are rendered with dimensional accuracy. Because the study concerns neck biomechanics, the geometry governing the mobility between each pair of cervical vertebrae was modeled in detail, with zygapophyseal facets reconstructed as complex 3D surfaces (15) that were precisely positioned and oriented with respect to their associated centra by 24 adjustable parameters for each vertebra. This degree of modeling permitted reconstruction of the limits of deflection attainable by each neck vertebra. The posture for the trunk and limbs was based on previous reconstructions and is not addressed here.

We modeled two well-known Late Jurassic sauropod taxa, *Apatosaurus* and *Diplodocus*. These genera were selected because they were close relatives (16–19) and were sympatric during the Late Jurassic (1, 2). Both genera are known from nearly complete skeletons [mounted Carnegie Museum of Natural

History (CM) specimens CM 3018 (*Apatosaurus louisae*) and CM 84 (*Diplodocus carnegii*)]. These specimens share the same number of neck vertebrae and have shorter forelimbs than hindlimbs, yet differ from one another in build and vertebral form.

The neutral pose and flexibility among cervical vertebrae was constrained by the placement, size, and 3D shape of their pre- and postzygapophyses. The movement of adjacent vertebrae, relative to the ball-and-socket articulations of the centra, induces rotation and translation of the articulated pre- and postzygapophyses. This movement places tension on the synovial capsule surrounding each zygapophyseal pair. Our manipulation of muscle and ligament preparations of extant bird necks indicated that synovial capsules constrain movement such that paired pre- and postzygapophyses could only be displaced to the point where the margin of one facet reaches roughly the midpoint of the other facet, at which point the capsule is stretched taut (20). In other words, one facet could slip upon the other until their overlap was reduced to about 50%. In vivo, muscles, ligaments, and fascia may have further limited movement (20); thus, the digital manipulations reported here represent a “best case” scenario for neck mobility.

We measured the cervical vertebrae of CM

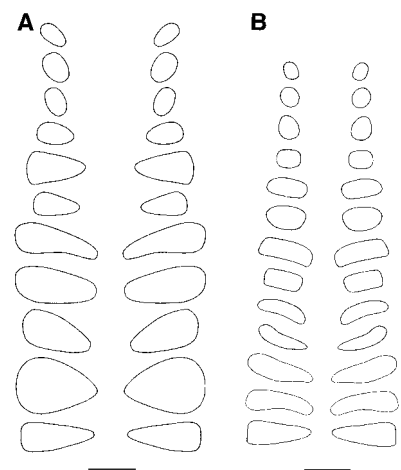


Fig. 1. Tracings of the articular facets of the prezygapophyses of (A) *Apatosaurus louisae* (specimen CM 3018) and (B) *Diplodocus carnegii* (specimen CM 84). Scale bars, 10 cm.

¹Computer and Information Science, University of Oregon, Eugene, OR 97403, USA. ²Biological Sciences, Northern Illinois University, DeKalb, IL 60115, USA.